

Mapping of linear and circular forms of mouse mammary tumor virus DNA with restriction endonucleases: Evidence for a large specific deletion occurring at high frequency during circularization

(agarose gel electrophoresis/molecular hybridization/RNA tumor viruses/proviral DNA)

PETER R. SHANK*, J. CRAIG COHEN*, HAROLD E. VARMUS*, KEITH R. YAMAMOTO†, AND GORDON M. RINGOLD†

* Department of Microbiology and † Department of Biochemistry and Biophysics, University of California, San Francisco, California 94143

Communicated by Norman Davidson, January 30, 1978

ABSTRACT Rat hepatoma cells infected with mouse mammary tumor virus contain multiple forms of unintegrated viral DNA when grown in the presence of glucocorticoids. Using the DNA transfer procedure of Southern, we have prepared restriction endonuclease fragment maps of these forms of viral DNA. The maps indicate that: (i) the major species of viral DNA is a linear molecule of 5.9×10^6 M, located in the cytoplasm; (ii) the nuclei contain covalently closed circular viral DNA of two distinct sizes (5.1×10^6 and 5.9×10^6 M_r) in addition to linear molecules (5.9×10^6 M_r); (iii) the linear molecule has specific termini; (iv) there is extensive homology between regions at or near termini of the linear molecule; (v) the predominant form of circular DNA lacks 1.2 kilobase pairs present in both the larger circular molecule and the linear molecule; and (vi) the sequences deleted from the majority of the circular DNA molecules are located at the ends of the linear DNA that are joined during circularization.

The mouse mammary tumor virus (MMTV) is unusual among RNA tumor viruses, because it causes carcinomas rather than leukemias or sarcomas (1, 2) and it displays dramatic regulation of transcription by glucocorticoid hormones (3, 4). Since the genome appears to replicate through a DNA provirus integrated covalently into host cell DNA, we are attempting to use restriction endonucleases to assess the influence of defined regions of the provirus and its integration sites upon carcinogenesis and steroidal regulation.

Cultured cells of various species can be infected by MMTV (5, 6); rat hepatoma cells that are chronically infected by MMTV and grown in the presence of dexamethasone contain multiple (10–20) copies of unintegrated viral DNA (7). Most of these molecules appear to be the same length as a subunit of viral RNA (ca 9000 bases), and a significant portion is found in a covalently closed circular form (7). In this report, we characterize the viral DNA in greater detail, employing the DNA transfer procedure of Southern (8) to locate viral DNA with virus-specific molecular hybridization reagents after electrophoresis in agarose gels.

METHODS

Isolation of DNA. A clone (M1.19) obtained from cultured rat hepatoma cells infected with the GR strain of MMTV (MMTV-GR) was the source of unintegrated viral DNA. Cells were grown for 48 hr in medium containing $1 \mu\text{M}$ dexamethasone; DNA was prepared from the cytoplasm and from the supernatant fraction of a Hirt precipitation of the nuclei (7). Cytoplasmic DNA was sedimented through a 5–20% neutral

sucrose gradient containing 20 mM Tris-HCl, pH 7.4/100 mM NaCl/1 mM EDTA (STE) for 15 hr at 20° in the SW 27 rotor at 25,000 rpm; the 15–20S region was pooled. Covalently closed circular viral DNA was isolated from the sodium dodecyl sulfate (NaDodSO₄)/NaCl supernatant fraction by banding in CsCl/propidium diiodide gradients (7). Viral DNA was recovered from preparative agarose gels by dissolving the gel slices in 7 M NaClO₄, adsorbing the DNA to hydroxylapatite, and precipitating the eluted DNA with cetyltrimethylammonium bromide.

Restriction Mapping Techniques. Restriction endonucleases *Sal* I, *Hpa* I, *Hind*III, *Bam*HI, *Kpn* I, *Xho* I, and *Xba* I were obtained from New England BioLabs (Beverly, MA). *Sma* I, *Eco*RI, *Bgl* II, and *Pst* I were generous gifts from E. Daniell, P. Greene, P. Bolivar, and W. Brown, respectively. DNA digestions were performed in 20- μl volumes of the buffers specified by New England BioLabs; extent of digestion was monitored by inclusion of plasmid pBR 313 DNA or bacteriophage λ DNA.

Viral 70S RNA was iodinated (9) (10^8 cpm/ μg), mixed with an equal volume of saturated CsSO₄, centrifuged for 60 hr at 33,000 rpm in the SW 50.1 rotor at 20°, dialyzed against STE, and extracted with phenol/chloroform. DNA complementary to the entire viral genome (cDNA_{rep}) or to specific size classes of viral RNA was synthesized by avian myeloblastosis virus reverse transcriptase with oligomers of calf thymus DNA as primers (10). The polymerase reaction was performed for 45 min at 37° in 50 mM Tris-HCl, pH 8.1/2 mM dithiothreitol/40 mM KCl/8 mM MgCl₂/200 μM dGTP, 200 μM dATP, 200 μM TTP/100–200 μCi of [α -³²P]dCTP (Amersham/Searle, 250 Ci/mmol)/1 mg of primers/1 μg of viral 35S RNA/and 70 units of avian myeloblastosis virus polymerase in a final volume of 250 μl . cDNA_{4–10S} and cDNA_{15–24S} were prepared similarly by using 4–10S and 15–24S polyadenylated viral RNA as templates. These RNAs were prepared from 70S RNA by denaturation and sedimentation in a 15–30% sucrose gradient in STE with 0.1% NaDodSO₄ (21 hr at 20°, 21,000 rpm in the SW 27 rotor) followed by two selections on a column of oligo(dT)-cellulose (T3, Collaborative Research). DNA complementary to the 3' region of the viral RNA (cDNA_{3'}) was prepared by using oligo(dT)_{12–18} to prime DNA synthesis on short (4–10S) poly(A)-containing viral RNA, as described for avian sarcoma virus (11).

After fractionation by electrophoresis in 0.8% (wt/vol) aga-

The costs of publication of this article were defrayed in part by the payment of page charges. This article must therefore be hereby marked "advertisement" in accordance with 18 U. S. C. §1734 solely to indicate this fact.

Abbreviations: MMTV, mouse mammary tumor virus; cDNA, complementary DNA; form I, covalently closed circular duplex DNA; form II, nicked circular duplex DNA; form III, linear duplex DNA; SSC, 150 mM NaCl/15 mM citrate; STE, 20 mM Tris-HCl (pH 7.4)/100 mM NaCl/1 mM EDTA; NaDodSO₄, sodium dodecyl sulfate.

rose gel according to the method of Helling *et al.* (12), DNA was transferred from the gel onto nitrocellulose sheets (Millipore Corp., HA WP) with $6\times$ SSC (SSC = 150 mM NaCl/15 mM Na citrate) (8). The filters were baked at 80° for 2 hr *in vacuo* and prehybridized for 6–18 hr at 41° in annealing mix [$3\times$ SSC, 50% (vol/vol) formamide, yeast RNA at 200 $\mu\text{g}/\text{ml}$, denatured salmon sperm DNA at 20 $\mu\text{g}/\text{ml}$] supplemented with Denhardt's buffer (13) containing 0.02% (wt/vol) each of bovine serum albumin, polyvinylpyrrolidone, and Ficoll. Hybridization with either RNA or cDNA was performed at 41° by saturating the filters (1 ml/100 cm^2) with an annealing mix containing 1×10^6 cpm/ml of the annealing reagent; the mix was supplemented with Denhardt's solution for the cDNA hybridization. The filters were then wrapped in SaranWrap and incubated for 48 hr. Unannealed cDNA was removed from the filters by washing once in 200 ml of $2\times$ SSC/ $1\times$ Denhardt's solution at 20° and then repeatedly (5–10 changes) for 24 hr in 200 ml of $6\times$ SSC/0.5% (wt/vol) NaDodSO₄ at 68° . Unannealed RNA was removed similarly except that only one 68° wash was performed (without NaDodSO₄) and the filters were then treated with a mixture of pancreatic and T1 ribonucleases (50 $\mu\text{g}/\text{ml}$ and 5 units/ml, respectively) in $2\times$ SSC at 37° for 30 min. In either case the filters were then washed twice in $2\times$ SSC at 20° , air dried, and exposed for 1–10 days at -70° to Kodak RP-ROYAL X-OMAT film in the presence of a Dupont Cronex "Lightning Plus" intensifying screen (14); these conditions detect ³²P 5-fold more efficiently than ¹²⁵I.

RESULTS

Size and Structure of Unintegrated MMTV DNA. M1.19 cells contain multiple copies of viral DNA integrated into the cellular genome; after growth in dexamethasone, the cells also contain 1–3 copies of closed circular viral DNA in the nucleus and 1–20 copies of linear (or open circular) viral DNA, located predominantly in the cytoplasm (7).

The size and structure of the unintegrated species were further examined by electrophoresis in an agarose gel followed by transfer to nitrocellulose filters and hybridization with ¹²⁵I-labeled viral RNA (Fig. 1). The cytoplasmic species of viral DNA was identified as a single band in the position expected for a linear (form III) duplex molecule of $5.9 \times 10^6 M_r$ (Fig. 1C) which is consistent with the idea that the linear DNA is a complete copy of a haploid subunit of the viral RNA genome [*ca* $3 \times 10^6 M_r$ (16, 17)].

Electrophoresis of closed circular (form I) DNA from nuclear fractions revealed two bands of DNA that migrated more rapidly than the linear DNA (Fig. 1A). To determine whether these two electrophoretic species differ in molecular weight or in superhelix density (18), the circular DNA was cleaved with *Eco*RI, a restriction enzyme that appears to recognize a single site in MMTV DNA (Fig. 2B, lane 11); the resulting products demonstrated mobilities expected for linear molecules of 5.9×10^6 and $5.1 \times 10^6 M_r$ (Fig. 1D). The closed circular structure of the nuclear DNA was further documented by the introduction of a limited number of nicks with DNase I in the presence of ethidium bromide. This procedure converted the two rapidly migrating species into open circular (form II) species that migrated more slowly than form I or form III molecules of the same M_r (Fig. 1B). [The three forms of pBR 313 plasmid DNA ($5.8 \times 10^6 M_r$) behaved similarly under our electrophoresis conditions.] Two additional points should be noted: first, in all methods of analysis of DNA isolated as form I (Fig. 1 A, B, and D), the smaller species ($5.1 \times 10^6 M_r$) was more abundant than the species with the size of the linear DNA; second, the efficiency of detection of all three forms of DNA was similar, indicating that under our conditions form I DNA

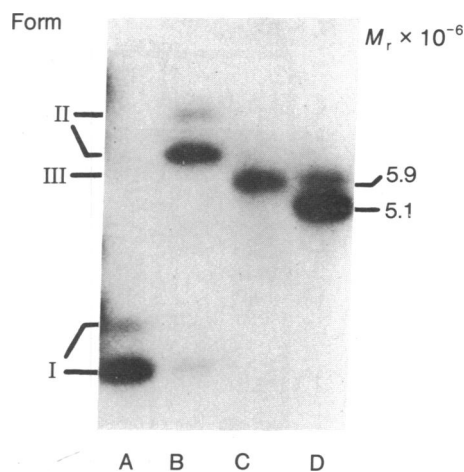


FIG. 1. Forms of unintegrated viral DNA from the cytoplasm and nucleus of M1.19 cells. Approximately 0.2 ng of viral DNA mixed with 0.2 μg of form I plasmid pBR 313 DNA was electrophoresed in a 0.8% (wt/vol) agarose gel. The gel was stained with ethidium bromide to visualize the internal markers (pBR 313 DNA and an *Eco*RI digest of λ DNA) in a parallel lane. The DNA was transferred onto a nitrocellulose sheet and annealed with ¹²⁵I-labeled viral RNA. Lanes: A, form I MMTV DNA; B, form I MMTV DNA digested with DNase I in the presence of ethidium bromide; C, cytoplasmic MMTV DNA; D, form I MMTV DNA digested with *Eco*RI.

was transferred to nitrocellulose as efficiently as form II or form III.

Mapping Fragments of MMTV DNA Generated by Restriction Enzymes. Eleven restriction endonucleases with hexanucleotide recognition sites were screened for their ability to cleave linear and circular MMTV DNA. Three enzymes (*Sal* I, *Sma* I, and *Hpa* I) did not cleave within viral DNA, four (*Eco*RI, *Hind*III, *Kpn* I, and *Xho* I) cleaved viral DNA once, and three (*Bam*HI, *Xba* I, and *Bgl* II) cleaved twice (see below). The remaining enzyme, *Pst* I, generated five fragments from linear DNA; these were used to compare the distribution of radioactivity among fragments when [³²P]cDNA_{rep} replaced ¹²⁵I-labeled RNA as a hybridization reagent (Fig. 2A). Since cDNA_{rep} detected all fragments and offered improved sensitivity, it was employed in all subsequent studies.

Three methods were used to produce a map of cleavage sites in MMTV-GR DNA (cf. Fig. 5): (i) comparison of digestion of the linear and the two species of circular viral DNA; (ii) sequential digestion with different enzymes; and (iii) isolation of specific restriction endonuclease fragments followed by digestion with a second enzyme.

(i) **Comparison of DNA species.** *Bam*HI digestion of unfractionated form I MMTV DNA produced three fragments of 5.2×10^6 , 4.4×10^6 , and $0.7 \times 10^6 M_r$ (Fig. 2B, lane 2); digestion of both of the separated form I molecules (Fig. 2B, lanes 3 and 4) yielded the smallest ($0.7 \times 10^6 M_r$) fragment, whereas the two larger fragments (5.2×10^6 and $4.4 \times 10^6 M_r$) were derived uniquely from form I molecules of each size. Digestion of the linear MMTV DNA with *Bam*HI produced three fragments of 3.8×10^6 , 1.4×10^6 , and $0.7 \times 10^6 M_r$ (Fig. 2B, lane 5), indicating the $0.7 \times 10^6 M_r$ fragment to be internal and the 3.8×10^6 and $1.4 \times 10^6 M_r$ *Bam*HI fragments to be terminal on the linear molecule. The $1.4 \times 10^6 M_r$ *Bam*HI fragment always appeared "under-represented" with respect to the $0.7 \times 10^6 M_r$ *Bam*HI fragment with cDNA_{rep} (see Fig. 2B, lanes 5–8; Fig. 2C). This under-representation was also evident, though to a lesser degree, when ¹²⁵I-labeled RNA was used as the annealing reagent (data not shown). However, the intensities of the *Bam*HI bands were roughly proportional to their size

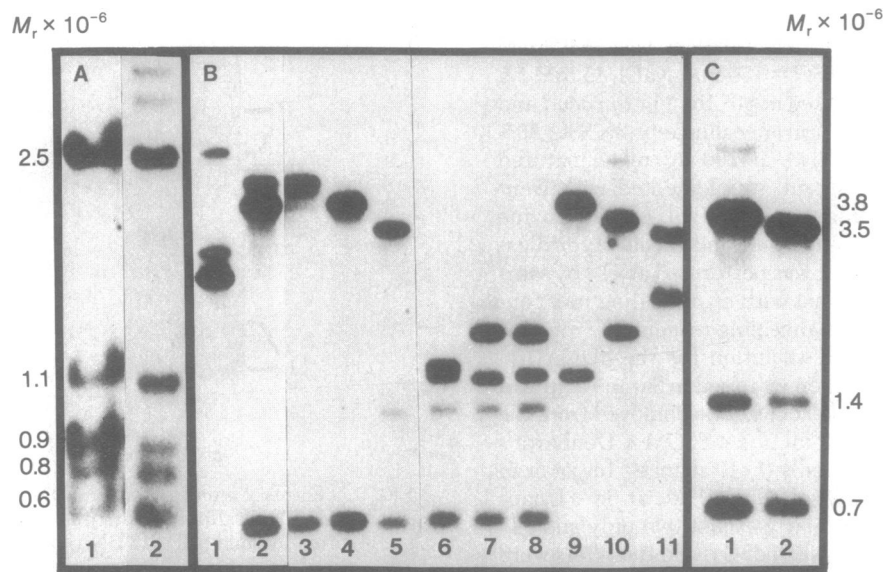


FIG. 2. Restriction endonuclease mapping of unintegrated MMTV DNA. Circular and linear forms of MMTV DNA from the cytoplasm and nucleus of M1.19 cells and large and small forms of circular DNA from a preparative agarose gel were digested with the indicated enzymes and subjected to electrophoresis in 0.8% (wt/vol) agarose gels and then analyzed. The gels in A were electrophoresed further than the gels shown in B and C. Molecular weights were determined by comparison with parallel lanes containing both an *EcoRI* digest of λ DNA and a *HindIII* digest of SV 40 DNA. (A) MMTV linear DNA was digested with *Pst* I and annealed with ^{125}I -labeled RNA (lane 1) or with ^{32}P cDNA_{rep} (lane 2). (B) Form I MMTV DNA (lane 1); *Bam*HI digestions of form I MMTV DNA, large circular MMTV DNA, small circular MMTV DNA, and linear MMTV DNA (lanes 2–5); sequential digestion of linear MMTV DNA with *Xba* I and *Bam*HI, *Kpn* I and *Bam*HI, *Xho* I and *Bam*HI (lanes 6–8); linear MMTV DNA digested with *Xho* I, *Kpn* I, and *Eco*RI (lanes 9–11). The filter was annealed with ^{32}P cDNA_{rep}. (C) Linear MMTV DNA digested with *Bam*HI (lane 1); linear MMTV DNA sequentially digested with *Bam*HI and *Eco*RI (lane 2). The filter was annealed with ^{32}P cDNA_{rep}.

when cDNA_{rep} was prepared by using ^{32}P dATP (rather than ^{32}P dCTP). The apparent under-representation of the $1.4 \times 10^6 M_r$ *Bam*HI fragment when detected with reagents labeled at cytosine residues could therefore be due to a relatively low concentration of deoxyguanine residues in this region of the viral DNA.

Similar analyses comparing linear and large circular DNA were done with *Bgl*II and *Pst* I (Fig. 3, F vs. G and I vs. J). The $2.4 \times 10^6 M_r$ *Bgl* II fragment was generated by cleavage of both circular and linear forms and thus must occupy an internal position on the linear map (cf. Fig. 5); the 2.7×10^6 and $0.8 \times 10^6 M_r$ *Bgl* II fragments represent the terminal regions linked in the large circular molecule to form a $3.5 \times 10^6 M_r$ fragment. *Pst* I digestion of both linear and large circular molecules gave identical patterns, indicating there must be a *Pst* I site close to one (or both) end of the linear DNA. Enzymes that cleave MMTV DNA once (*Eco*RI, *Xho* I, *Kpn* I, and *Hind*III) produce a linear molecule from each type of the form I molecules (see Fig. 1D) and two fragments from the linear molecule (Fig. 2B, lanes 9–11).

(ii) *Sequential digestions.* Sequential digestions with *Kpn* I and *Bam*HI (Fig. 2B, lane 7), *Xho* I and *Bam*HI (Fig. 2B, lane 8), and *Eco*RI and *Bam*HI (Fig. 2C, lane 2) located the sites for *Kpn* I, *Xho* I, and *Eco*RI with respect to the sites for *Bam*HI in linear DNA (we have arbitrarily drawn the $1.5 \times 10^6 M_r$ *Bam*HI fragment on the right side of the linear map; see Fig. 5B). Similar analyses with *Hind*III placed its cleavage site approximately 200 bases to the right of the *Eco*RI site (data not shown). Sequential digestion of linear DNA with *Bgl* II and *Bam*HI indicated that both *Bam*HI sites are within the $2.4 \times 10^6 M_r$ *Bgl* II fragment (data not shown), thereby ordering the *Bgl* II fragments with respect to the *Bam*HI map (cf. Fig. 5B).

Xba I digestion of large circular DNA produced fragments of 5.6×10^6 and $0.3 \times 10^6 M_r$ (data not shown). The size of the

four large fragments observed after sequential digestion of linear DNA with *Xba* I and *Bam*HI indicated that both *Xba* I sites are within the $3.8 \times 10^6 M_r$ *Bam*HI fragment (Fig. 2B, lane 6; the $0.3 \times 10^6 M_r$ *Xba* I fragment was not included in this gel). To determine the order of the two largest *Xba* I-*Bam*HI fragments (1.7 and $1.8 \times 10^6 M_r$), linear DNA was digested sequentially with *Xba* I, *Bam*HI, and *Eco*RI. The $1.7 \times 10^6 M_r$ fragment was found to contain the *Eco*RI site and is therefore located to the right of the $1.8 \times 10^6 M_r$ fragment (data not shown; cf. Fig. 5B).

(iii) *Recleavage of isolated fragments.* Sequential digestions of linear DNA with *Pst* I and *Bam*HI indicated that one *Bam*HI site is in the middle of the $1.1 \times 10^6 M_r$ *Pst* I fragment; *Pst* I and *Eco*RI digestion indicated that the *Eco*RI site is approximately $0.4 \times 10^6 M_r$ from one end of the $2.5 \times 10^6 M_r$ *Pst* I fragment (data not shown). These results locate the two largest *Pst* I fragments (2.5×10^6 and $1.1 \times 10^6 M_r$) on the physical map, but they do not position the three smaller *Pst* I fragments. We therefore digested linear DNA with *Eco*RI and separated the two fragments on a preparative agarose gel. The larger *Eco*RI fragment was contaminated with the smaller fragment, but the smaller fragment was quite pure (Fig. 3C). Digestion of the smaller (or right-hand) *Eco*RI fragment with *Pst* I (Fig. 3D) produced fragments of 1.1×10^6 , 0.8×10^6 , and $0.4 \times 10^6 M_r$. These data place the $0.8 \times 10^6 M_r$ *Pst* I fragment at the right-hand end of the linear map (Fig. 5C). Unfortunately, none of the other enzymes tested cleaved within $1.5 \times 10^6 M_r$ of the left-hand portion of the linear molecule; thus, we cannot establish the order of the 0.6 and $0.9 \times 10^6 M_r$ *Pst* I fragments (cf. Fig. 5).

Orientation of MMTV DNA with Respect to Viral RNA. To orient the DNA map (Fig. 5) with respect to the ends of the viral RNA, we annealed a cDNA_{3'} [complementary to the 200–300 nucleotides adjacent to the poly(A) at the 3' end of the viral RNA] to the *Pst* I fragments of linear MMTV DNA. Both

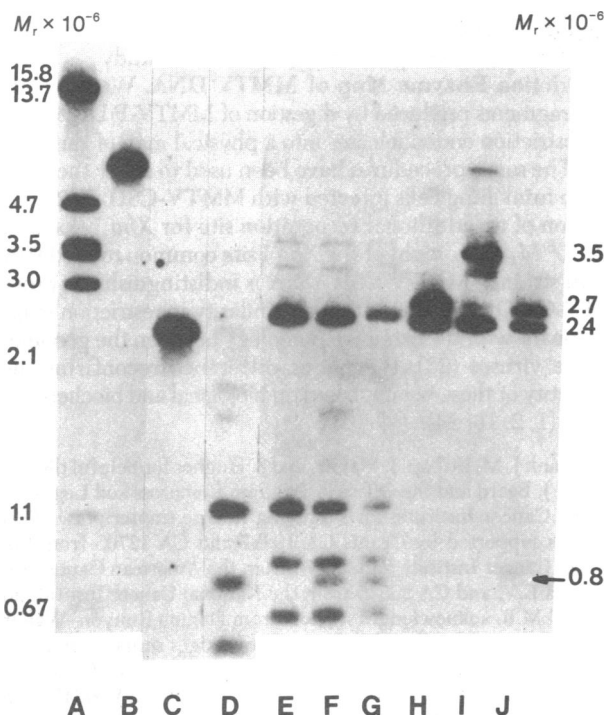


Fig. 3. Digestion of separated *EcoRI* fragments of linear MMTV DNA with *Pst* I and mapping of the region absent in the small MMTV circular DNA. The smaller of two *EcoRI* fragments from MMTV linear DNA (cf. Fig. 2B, lane 11), intact linear DNA, and both small and large species of form I MMTV were digested with *Pst* I or *Bgl* II and analyzed by annealing with $[^{32}\text{P}]\text{cDNA}_{\text{rep}}$ after electrophoresis in 0.8% (wt/vol) agarose gels. Lanes: A, marker *EcoRI* digest of λ $[^{32}\text{P}]\text{DNA}$ and *Hind*III digest of SV 40 $[^{14}\text{C}]\text{DNA}$; B, MMTV linear DNA; C, $2.3 \times 10^6 M_r$ *EcoRI* fragment; D, *Pst* I digestion of the smaller *EcoRI* fragment; E, smaller circular MMTV DNA digested with *Pst* I; F, large circular MMTV DNA digested with *Pst* I; G, linear MMTV DNA digested with *Pst* I (the two faint bands of approximately $3.5 \times 10^6 M_r$ in the *Pst* I digestions represent partial digestion products); H, small circular DNA digested with *Bgl* II; I, large circular MMTV DNA digested with *Bgl* II (the bands at the position of form I DNA and form III DNA represent incomplete digestion products not present in other digestions); J, linear MMTV DNA digested with *Bgl* II (the arrow indicates the position of the $0.8 \times 10^6 M_r$ fragment).

the 0.8×10^6 and $0.9 \times 10^6 M_r$ fragments were detected (Fig. 4A). These fragments have been mapped to opposite sides of the linear DNA, which suggests that sequences near the 3' end of the viral RNA, and represented in cDNA_3 , are repeated elsewhere in the viral DNA (see Discussion). We reasoned that the orientation of the DNA map could still be established, despite the redundancy of 3' sequences in the *Pst* I fragments, if reagents representing larger portions of the 3' half of the genome annealed with one or two, but not all three, of the remaining *Pst* I fragments. We prepared cDNAs from two size classes of poly(A)-selected RNA (see Materials and Methods); $\text{cDNA}_{4-10\text{S}}$ annealed to both the 0.8×10^6 and $0.9 \times 10^6 M_r$ *Pst* I fragments of linear DNA (Fig. 4B), confirming the results with the cDNA_3 . In contrast, $\text{cDNA}_{15-24\text{S}}$ annealed to the 1.1×10^6 and $2.5 \times 10^6 M_r$ *Pst* I fragments in addition to the 0.8 and $0.9 \times 10^6 M_r$ fragments (Fig. 4C), but it annealed little if at all to the $0.6 \times 10^6 M_r$ *Pst* I fragment (Fig. 4D). We therefore conclude that the right-hand side of the MMTV DNA map (Fig. 5) corresponds to sequences from the 3' end of the viral RNA.

Mapping the Deletion Present in the Major Form I Species of MMTV DNA. To determine whether the smaller form I

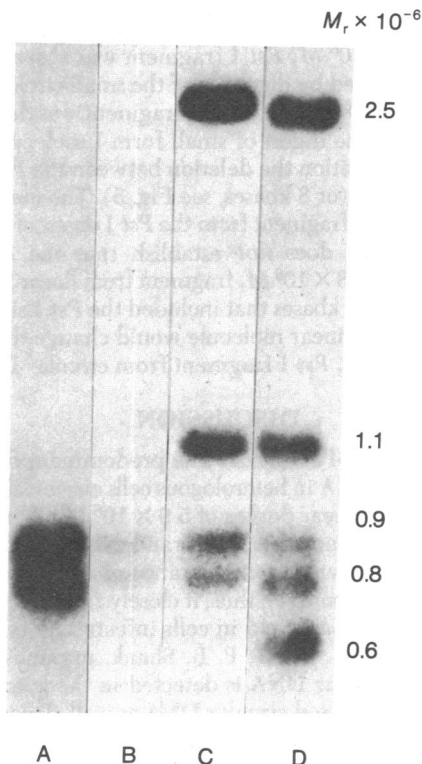


FIG. 4. Correlation of the *Pst* I fragments of linear DNA with viral RNA. Linear MMTV DNA was digested with *Pst* I and electrophoresed in a 0.8% (wt/vol) agarose gel. A parallel lane contained an *EcoRI* digest of λ $[^{32}\text{P}]\text{DNA}$ and a *Hind*III digest of simian virus 40 $[^{14}\text{C}]\text{DNA}$. After transfer onto nitrocellulose, the membrane was cut in order to anneal DNA in the four lanes with the indicated species of $[^{32}\text{P}]\text{cDNA}$. Lanes: A, cDNA_3 ; B, $\text{cDNA}_{4-10\text{S}}$; C, $\text{cDNA}_{15-24\text{S}}$; D, cDNA_{rep} .

molecules represent a deletion of specific sequences present in both the linear and the large form I molecules, we compared *Pst* I and *Bgl* II digests of small form I MMTV DNA with di-

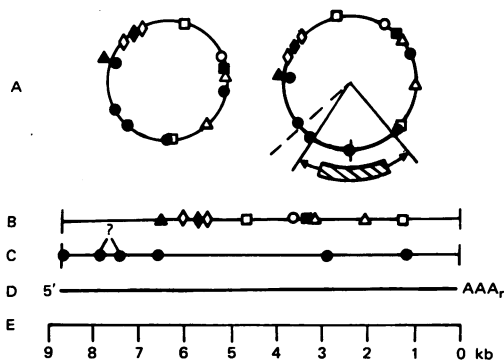


FIG. 5. Physical map of restriction endonuclease sites in unintegrated MMTV DNA. (A) Small and large circular MMTV DNA. The hatched area represents the 1.2-kbase (kb) deletion that may occur anywhere in the arc drawn between the *Pst* I (O) sites at 1.2 kb and 7.5 kb (or 8 kb; see C) as long as it encompasses the *Pst* I site at the end(s) of the linear DNA molecule. The *EcoRI* (O), *Xba* I (\diamond), *Bam*HI (Δ), *Bgl* II (\square), *Hind*III (\blacksquare), *Xho* I (\blacktriangle), and *Kpn* I (\blacklozenge) cleavage sites are indicated. (B) Linear MMTV DNA. (C) Linear MMTV DNA with the *Pst* I cleavage sites indicated. Our data do not unambiguously determine the position of the *Pst* I site near the left-hand end of the linear molecule (indicated by a question mark) and do not indicate whether there are *Pst* I sites at both ends or only at one end of the linear DNA (the latter possibility is drawn). (D) Viral RNA drawn to correlate with the linear DNA (see Discussion). Thus, the left-hand half of the map represents the 5' half of the RNA. (E) Scale in kilobases.

gests of linear and large circular DNAs (Fig. 3E-G and H-J). The $0.8 \times 10^6 M_r$ *Pst* I fragment was absent from the fragments generated by digestion of the small circle (Fig. 3E). Similarly, the $3.5 \times 10^6 M_r$ *Bgl* II fragment was decreased to $2.7 \times 10^6 M_r$ in the digest of small form I molecules (Fig. 3H). These data position the deletion between the *Pst* I sites at 1.2 and 7.5 kbases (or 8 kbases, see Fig. 5). The mere absence of an $0.8 \times 10^6 M_r$ fragment from the *Pst* I digest of small form I DNA (Fig. 3E) does *not* establish that the deletion is colinear with the $0.8 \times 10^6 M_r$ fragment from linear DNA, since any deletion of 1.2 kbases that included the *Pst* I site (or sites) at the ends of the linear molecule would change the mobility of the $0.8 \times 10^6 M_r$ *Pst* I fragment from circular DNA.

DISCUSSION

Structure of MMTV DNA. The predominant form of un-integrated viral DNA in heterologous cells chronically infected with MMTV is a linear duplex of $5.9 \times 10^6 M_r$. This molecule is composed of a genome-length strand complementary to the viral genome and subgenomic strands of the same chemical polarity as the genome (7); thus, it closely resembles the major species of viral DNA found in cells infected by type C RNA tumor viruses (refs. 19-21; P. R. Shank, unpublished data). Although only linear DNA is detected in the cytoplasm, the nucleus contains closed circular DNA as well. Two size classes of circular DNA have been observed, a minor one of $5.9 \times 10^6 M_r$ and a major one of $5.1 \times 10^6 M_r$. Linear and circular viral DNA molecules of these sizes have also been observed in mink lung cells infected with the strain of MMTV isolated from C3H mice (MMTV-C3H) (unpublished data).

Our mapping studies demonstrate that the smaller circles lack about 1.2 kilobase pairs present in the larger circles; the deleted sequences are located near the ends of the linear molecule (Figs. 3 and 5). In cells infected by avian sarcoma virus, pulse-chase experiments have established directly that the cytoplasmic linear DNA is precursor to closed circular DNA in the nucleus (21). Thus, we suggest that the small molecules may arise by aberrant circularization of the linear DNA, but we do not know the mechanism or the significance of this event. Similar, though smaller, deletions at or near the ends of the linear DNA occur in the circular DNA of avian sarcoma virus (P. R. Shank, unpublished data) and murine leukemia virus (F. Yoshimura and R. A. Weinberg, personal communication).

Orientation of the Viral DNA with Respect to the RNA Genome. Digestion of linear DNA with restriction enzymes demonstrates that molecules are not circularly permuted. Analysis of *Pst* I digests of linear viral DNA by hybridization with cDNAs representing different regions of the RNA genome suggests that the right-hand portion of the restriction endonuclease map (Fig. 5) represents the 3' end of the viral RNA. It is unlikely, however, that the termini correspond exactly to the ends of the viral RNA. In all cases of RNA tumor viruses examined thus far, the primer for DNA synthesis by reverse transcriptase is a tRNA species located within 100-200 bases of the 5' terminus of the genome (22); preliminary evidence with MMTV indicates the primer is approximately 130 bases from the 5' end (J. Majors, personal communication). Since DNA synthesis presumably continues on a 3' terminus after transfer of the polymerase from the 5' terminus, the proximal end of the resulting linear DNA is probably permuted approximately 130 bases with respect to the viral RNA. The precise nature of the distal end of the linear DNA is unknown. However, the studies reported here with cDNA_{3'}, as well as unpublished data with cDNA specific for the 5' region, indicate

that redundancies are present in the linear DNA; the location and nature of these sequences require further study.

Restriction Enzyme Map of MMTV DNA. We have ordered fragments produced by digestion of MMTV-P DNA with eight restriction endonucleases into a physical map of the viral DNA. The same procedures have been used to study the viral DNA in mink lung cells infected with MMTV-C3H. With the exception of an additional recognition site for *Xho* I (located $0.3 \times 10^6 M_r$ to the right of the *Xho* I site common to the DNA of both strains), MMTV-C3H DNA is indistinguishable from MMTV-GR DNA in our tests. The similarity in restriction maps is consonant with the extensive homology between the genomes of these viruses (23); the minor difference reconfirms the nonidentity of these isolates based on biological and biochemical criteria (1, 2, 16, 24).

We thank J. M. Bishop, J. Majors, and S. Hughes for helpful discussions and J. Beard and the Office of Program Resources and Logistics, National Cancer Institute, for supplying reverse transcriptase. This work was supported by Grants CA 19287 and CA 12705 from the National Cancer Institute and VC 70 from the American Cancer Society to H.E.V. and CA 20535 from the National Cancer Institute to K.R.Y.; G.M.R. acknowledges support from Damon Runyon-Walter Winchell Cancer Fund and J.C.C. acknowledges support from the California Division of the American Cancer Society (J-330C). K.R.Y. is recipient of Research Career Development Award CA 00347 from the National Cancer Institute.

- Nandi, S. & McGrath, C. M. (1973) *Adv. Cancer Res.* **17**, 353-414.
- Moore, D. H. (1975) in *Cancer: A Comprehensive Treatise*, ed. Becker, F. F. (Plenum, New York), Vol. 2, pp. 131-167.
- Parks, W. P., Scolnick, E. M. & Kozikowski, E. H. (1974) *Science* **184**, 158-160.
- Ringold, G. M., Yamamoto, K. R., Tomkins, G. M., Bishop, J. M. & Varmus, H. E. (1975) *Cell* **6**, 299-305.
- Vaidya, A. B., Lasfargues, E. Y., Heubel, G., Lasfargues, J. C. & Moore, D. H. (1976) *J. Virol.* **18**, 911-917.
- Ringold, G. M., Cardiff, R. D., Varmus, H. E. & Yamamoto, K. R. (1977) *Cell* **10**, 11-18.
- Ringold, G. M., Yamamoto, K. R., Shank, P. R. & Varmus, H. E. (1977) *Cell* **10**, 19-26.
- Southern, E. M. (1975) *J. Mol. Biol.* **38**, 503-517.
- Commerford, S. L. (1971) *Biochemistry* **10**, 1993-1999.
- Taylor, J. M., Illmensee, R. & Summers, S. (1976) *Biochim. Biophys. Acta* **442**, 324-330.
- Tal, J., Kung, H. J., Varmus, H. E. & Bishop, J. M. (1977) *Virology* **79**, 183-197.
- Helling, R. B., Goodman, H. M. & Boyer, H. W. (1974) *J. Virol.* **14**, 1235-1244.
- Denhardt, D. T. (1966) *Biochem. Biophys. Res. Commun.* **23**, 641-646.
- Swanstrom, R. & Shank, P. R. (1978) *Anal. Biochem.*, in press.
- Cardiff, R. D. & Duesberg, P. H. (1968) *Virology* **36**, 696-700.
- Friedrich, R., Morris, V., Goodman, H. M., Bishop, J. M. & Varmus, H. E. (1976) *Virology* **72**, 330-340.
- Keller, W. & Wendel, I. (1974) *Cold Spring Harbor Symp. on Quant. Biol.* **39**, 199-208.
- Canaani, E., Duesberg, P. & Dina, D. (1977) *Proc. Natl. Acad. Sci. USA* **74**, 29-33.
- Smotkin, D., Yoshimura, F. K. & Weinberg, R. A. (1976) *J. Virol.* **20**, 621-629.
- Fritsch, E. & Temin, H. M. (1977) *J. Virol.* **21**, 119-130.
- Shank, P. R. & Varmus, H. E. (1978) *J. Virol.* **25**, 104-114.
- Taylor, J. M. (1977) *Biochim. Biophys. Acta* **473**, 57-71.
- Ringold, G. M., Blair, P. B., Bishop, J. M. & Varmus, H. E. (1976) *Virology* **70**, 550-553.
- Teramoto, Y. A., Kufe, D. & Schlom, J. (1977) *Proc. Natl. Acad. Sci. USA* **74**, 3564-3568.